CHEMMEDCHEM

DOI: 10.1002/cmdc.200800051

Substrate-Induced Stable Enzyme–Inhibitor Complex Formation Allows Tight Binding of Novel 2-Aminopyrimidin-4(3*H*)-ones to Drug-Resistant HIV-1 Reverse Transcriptase Mutants

Alberta Samuele,[b] Marcella Facchini,[b] Dante Rotili,[a] Antonello Mai,*[a] Marino Artico,[a] Mercedes Armand-Ugón,[c] José A. Esté,[c] and Giovanni Maga*[b]

*We recently reported the synthesis and biological evaluation of a novel series of 5-alkyl-2-(*N,N*-disubstituted)amino-6-(2,6-difluorophenylalkyl)-3,4-dihydropyrimidin-4(3*H*)-ones (F*2*-N,N-DABOs). These compounds are highly active against both wild-type HIV-1 and the K103N, Y181C, and Y188L mutant strains. Herein we present novel 6-(2-chloro-6-fluorophenylalkyl)-N,N-DABO (2-Cl-6-F-N,N-DABO) derivatives and investigate the molecular basis for their high-affinity binding to HIV-1 reverse transcriptase (RT). Our results show that the new compounds display higher association rates than the difluoro derivatives toward wild-type HIV-1 RT or drug-resistant RT mutant forms. We also show that they preferentially associate to either the free enzyme or the enzyme–nucleic acid binary complex, and that this binding is stabilized upon formation of the ternary complex between HIV-1 RT and both the nucleic acid and nucleotide substrates. Interestingly, one compound showed dissociation rates from the ternary complex with RT mutants K103N and Y181I 10–20-fold slower than from the corresponding complex with wild-type RT.*

Introduction

Human immunodeficiency virus (HIV) is the etiological agent of acquired immunodeficiency syndrome (AIDS). The current therapy against AIDS is based on four classes of anti-HIV drugs: nucleoside and nucleotide reverse transcriptase (RT) inhibitors (NRTIs and NtRTIs, respectively), non-nucleoside reverse transcriptase inhibitors (NNRTIs), protease inhibitors (PIs), and the fusion inhibitor (FI) enfuvirtide.[1] Despite their low toxicity and favorable pharmacokinetic properties, the use of first-generation NNRTIs both in monotherapy and in multidrug anti-AIDS cocktails has led to the rapid emergence of drug resistance. As a consequence, efforts are now focused on the development of novel compounds endowed with higher anti-HIV-1 activity and a resistance profile different from that of known drugs (second-generation NNRTIs). Continuous efforts in this field are documented by the large number of NNRTIs recently described in the literature, some of which are under clinical trials.

Dihydroalkoxybenzyloxopyrimidines (DABOs) were disclosed by our research group in 1992 as a novel NNRTI class.[2] Since then, a great number of oxopyrimidines have been synthesized and tested as anti-HIV-1 agents to obtain more potent and selective compounds. Structure–activity relationship (SAR) profiles of DABOs together with molecular modeling investigations of their putative binding modes have shown that the presence of a C2-alkoxy (DABOs),[3–5] -alkylthio (S-DABOs),[6–9] or -alkylamino (NH-DABOs)[10,11] side chain is a structural determinant for the antiviral activity of these derivatives. Moreover, 2,6-difluoro substitution on the C6-phenylmethyl moiety and the introduction of a methyl group at the pyrimidine C5-position and on the methylene bridge that connects the pyrimidine and phenyl rings (benzylic position) furnished new conformationally restricted compounds with nanomolar activity against wild-type HIV-1 and sub-micromolar activity against the Y181C mutant strain.[8–11] Cross-docking experiments performed by us on 68 different NNRTI–RT complexes suggested that a double N,N substitution on the 2-amino-DABO template can confer an implicit increased capacity for the molecules to re-adopt different experimental non-nucleoside binding site (NNBS) conformations by preventing the C2-NH group from establishing a further hydrogen bond in the NNBS. This information potentially leads to more flexible RT inhibitors with a broader range of activity against NNRTI-resistant mutants.[12] This hypothesis was confirmed by the synthesis and characterization of 2,6-difluoro-substituted N,N-DABO derivatives, which proved to be superior to the corresponding NH-DABOs both in

[a] *Dr. D. Rotili, Prof. A. Mai, Prof. M. Artico*
Istituto Pasteur—Fondazione Cenci Bolognetti
Dipartimento di Studi Farmaceutici, Sapienza Università di Roma
P.le A. Moro 5, 00185 Roma (Italy)
Fax: (+39) 06-491-491
E-mail: antonello.mai@uniroma1.it

[b] *Dr. A. Samuele, Dr. M. Facchini, Dr. G. Maga*
Istituto di Genetica Molecolare IGM-CNR
via Abbiategrasso 207, 27100 Pavia (Italy)
Fax: (+39) 0382-422-286
E-mail: maga@igm.cnr.it

[c] *Dr. M. Armand-Ugón, Dr. J. A. Esté*
Retrovirology Laboratory IrsiCaixa
Hospital Universitari Germans Trias i Pujol
Universitat Autònoma de Barcelona, 08916 Badalona (Spain)

terms of antiviral potency and in their activity spectrum toward drug-resistant mutants.[13,14]

We have previously shown that 2,6-F_2-*N*,*N*-DABO derivatives owe their potent inhibitory activity to their very high affinity for the NNBS.[13] However, their kinetics showed low association rates to HIV-1 RT, behaving as slow-binding/high-affinity inhibitors. To overcome this limitation, we explored a series of derivatives and evaluated them for their ability to interact with wild-type and mutant HIV-1 RT forms. Herein we report the discovery of 2-Cl-6-F-*N*,*N*-DABO derivatives, which show rapid association coupled with high-affinity binding to HIV-1 RT. Moreover, these novel compounds display a unique mode of action, resulting in higher-affinity binding to the K103N and Y181I RT mutants than to the wild-type enzyme.

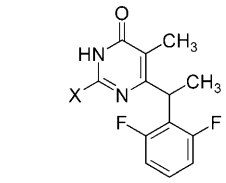

2,6-F_2-*N*,*N*-DABOs

MC1220 X = NMe_2
MC1236 X = piperidin-1-yl
MC1281 X = thiomorpholin-4-yl

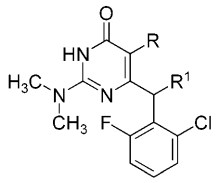

2-Cl-6-F-*N*,*N*-DABOs

MC1778 R = R^1 = H
MC1784 R = Me; R^1 = H
MC1838 R = H; R^1 = Me
MC1839 R = R^1 = Me

Figure 1. Structures of 2,6-F_2-*N*,*N*-DABOs and 2-Cl-6-F-*N*,*N*-DABOs.

Results and Discussion

2-Cl-6-F-*N*,*N*-DABO derivatives show improved activity against HIV-1 RT relative to 2,6-F_2-*N*,*N*-DABOs

The 2-Cl-6-F-*N*,*N*-DABOs were prepared following our reported procedures,[13,14] starting from 2-chloro-6-fluorophenylacetic or -phenylpropionic acid with a) *N*,*N*′-carbonyldiimidazole, b) potassium ethyl malonate or 2-methylmalonate in the presence of triethylamine and magnesium chloride, followed by acidic hydrolysis, and c) condensation of the obtained β-oxoesters with *N*,*N*-dimethylguanidine sulfate in the presence of sodium ethoxide (Scheme 1). Compounds MC1838 and MC1839, which

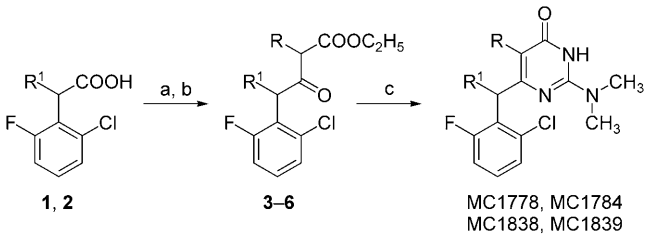

Scheme 1. Reagents and conditions: a) *N*,*N*′-carbonyldiimidazole, CH_3CN, room temperature; b) 1) $KOOCCHRCOOC_2H_5$, $MgCl_2$, $(C_2H_5)_3N$, CH_3CN, room temperature, 2) 4 N HCl, room temperature; c) *N*,*N*-dimethylguanidine hydrogensulfate, C_2H_5ONa, C_2H_5OH, reflux.

share a chiral center at the benzylic position, were prepared and tested as racemates. In previous DABO studies,[9–11,15] the *R* enantiomer of related derivatives was predicted as the most active; studies are in progress to confirm this hypothesis for this series as well.

The inhibitory potencies (K_i values) of the 2-Cl-6-F-*N*,*N*-DABO derivatives MC1778, MC1784, MC1838, and MC1839 (Figure 1) were compared with those of the 2,6-F_2 derivatives MC1220, MC1236, and MC1281 against wild-type and drug-resistant recombinant HIV-1 RT. The data are summarized in Table 1. It can be observed that the presence of two methyl groups at the pyrimidine C5-position (R) and on the methylene bridge that connects the pyrimidine and phenyl rings (benzylic position, R_1) (Figure 1) imparts the 2-Cl-6-F derivative MC1839 with greater activity toward wild-type RT and the Y181I mutant than

Table 1. Inhibitory potencies of *N*,*N*-DABOs against wild-type and mutated HIV-1 RT forms.

Compd	K_i [μM][a]		
	Wild Type	K103N	Y181I
MC1220	0.1 ± 0.03	0.5 ± 0.1	4.0 ± 0.5
MC1236	0.07 ± 0.01	0.60 ± 0.05	NA[b]
MC1281	0.06 ± 0.01	10.0 ± 1.12	NA
MC1778	0.712 ± 0.06	14.000 ± 1.54	NA
MC1784	0.307 ± 0.03	15.000 ± 1.63	NA
MC1838	0.003 ± 0.0002	1.00 ± 0.09	6.04 ± 0.59
MC1839	0.017 ± 0.001	0.75 ± 0.08	0.42 ± 0.04

[a] K_i values were determined with a fixed pre-incubation time of 10 min for all compounds. Numbers are the mean of three independent estimates ± SD. [b] NA: not active up to a final concentration of 20 μM.

the tested 2,6-F_2 derivatives. Interestingly, replacement of the methyl group at position R with a hydrogen atom (compound MC1838), gives a further increase in activity toward the wild-type enzyme, but a significant loss of potency against the Y181I mutant. As for the K103N mutant, the 2-Cl-6-F-*N*,*N*-DABOs MC1838 and MC1839 showed the same range of activity as the 2,6-F_2 derivatives MC1220 and MC1236, and were much more potent than MC1281. Interestingly, replacement of either one or both methyl groups with a hydrogen atom (such that R^1 = H), the respective thymine and uracil derivatives MC1784 and MC1778 showed an evident loss of potency against all RT forms tested. Cellular data (Table 2) confirmed the increased potency of the 6-(2-phenylethyl) and 5-methyl-6-(2-phenylethyl)-2-chloro-6-fluoro-*N*,*N*-DABO derivatives MC1838 and MC1839 relative to the corresponding uracil and thymine counterparts (MC1778 and MC1784, respectively). Regarding the 2,6-F_2-*N*,*N*-DABOs, MC1838 and MC1839 displayed the same (MC1220) or greater (MC1236 and MC1281) activities against the wild-type HIV-1 NL4-3 strain, and showed an inhibitor profile against the clinical isolate IRLL98 (containing multiple drug-resistance mutations to both NRTIs and NNRTIs) and the clinically relevant mutant strains K103N, Y181C, and Y188L similar to those of MC1236 and MC1281, whereas MC1220 was more potent. The two 2-Cl-6-F-*N*,*N*-DABO derivatives that displayed the best activity in their class, MC1838 and MC1839, were selected for further mechanistic studies.

Table 2. Cytotoxicity and anti-HIV-1 activity of *N*,*N*-DABOs.[a]

Compd	CC_{50} [μM][b]	EC_{50} [μM][c] NL4-3 (WT)	IRLL98[d]	K103N	Y181C	Y188L
MC1220	>17[e]	0.0003±0.0001	0.005±0.001	0.05±0.01	0.014±0.001	0.05±0.01
MC1236	>75	0.007±0.001	0.06±0.01	0.52±0.01	0.07±0.01	0.39±0.01
MC1281	>71	0.003±0.0005	0.06±0.01	1.24±0.01	0.03±0.005	0.86±0.01
MC1778	>3.5	0.062±0.001	ND[f]	ND	ND	ND
MC1784	>423	1.35±0.01	ND	ND	ND	ND
MC1838	>85	0.0007±0.0001	0.056±0.001	0.78±0.01	0.068±0.001	1.66±0.01
MC1839	>2	0.0003±0.00005	0.03±0.01	0.13±0.01	0.11±0.01	0.72±0.01

[a] Values are means ±SD determined from at least two experiments; a brief description of the assays is reported in the Experimental Section. [b] Cytotoxic concentration 50: concentration required to induce 50% death of non-infected cells, evaluated with the MTT method in MT-4 cells. [c] Effective concentration 50: concentration needed to inhibit 50% HIV-induced cytopathic effect, evaluated with the MTT method in MT-4 cells. [d] Clinical isolate resistant to NRTIs (lamivudine, emtricitabine) and NNRTIs (nevirapine, delavirdine, efavirenz). [e] Higher concentrations could not be achieved owing to precipitation of compounds in the culture medium. [f] ND: not determined.

2-Cl-6-F-*N*,*N*-DABO derivatives are not slow-binding inhibitors of HIV-1 RT

We have previously shown that the 2,6-F_2-*N*,*N*-DABO derivatives display a time-dependent increase in their inhibitory activity, characteristic of a slow-binding mechanism of inhibition. As shown in Figure 2A, the 2,6-F_2-*N*,*N*-DABOs MC1220, MC1236, and MC1281 increased their activity toward wild-type RT in a time-dependent fashion, as expected. We then tested whether the same was true for the most potent 2-Cl-6-F-*N*,*N*-derivatives, namely MC1838 and MC1839. Figure 2A shows the variations in the 50% inhibitory dose (ID_{50}) against wild-type HIV-1 RT for each compound as a function of pre-incubation time. As can be observed, no appreciable decrease in the inhibitory potencies of the 2-Cl-6-F compounds MC1838 and MC1839 was noted upon pre-incubation with the target enzyme, suggesting that these derivatives are not slow-binding inhibitors. The same behavior was noted against the drug-resistant mutant K103N (data not shown).

Binding kinetics of 2-Cl-6-F-*N*,*N*-DABO derivatives to wild-type and mutant HIV-1 RT relative to 2,6-F_2-*N*,*N*-DABOs

The rates of association (k_{on}) and dissociation (k_{off}) for the binding of the various inhibitors to all three catalytic states of HIV-RT (free enzyme, binary complex, and ternary complex) were determined. The calculated values are listed in Table 3. The 2-Cl-6-F derivatives showed 100–900-fold greater k_{on} values for all three states (free, binary, and ternary complexes) of wild-type HIV-1 RT, indicative of faster association relative to the 2,6-F_2-*N*,*N*-DABOs (Figure 2B and Table 3), thus explaining the lack of time-dependent inhibition for these compounds (Figure 2A). The 2-Cl-6-F derivatives MC1838 and MC1839 showed higher association rates than MC1220, MC1236, and MC1281 to all three states of the K103N mutant as well (Figure 2B and Table 3). Interestingly, compound MC1839 showed a lower dissociation rate from all the enzymatic states of the K103N mutated enzyme with respect to wild-type RT, whereas all the other compounds showed similar or higher k_{off} values for the mutant (Table 3). The 2,6-F_2-*N*,*N*-DABO MC1220 and the 2-Cl-6-F derivatives MC1838 and MC1839 were the only compounds that inhibit Y181I (Table 1). MC1838 and MC1839 again showed higher association rates than MC1220 toward all the states of this mutant (Figure 2B and Table 3). Furthermore, while MC1220 dissociated 66-fold faster from the mutant than from wild-type RT, the dissociation rate of MC1838 was not affected by the mutation, whereas MC1839 dissociated more slowly from all three states (free, binary, and ternary complexes) of the Y181I mutant than from the wild type. These

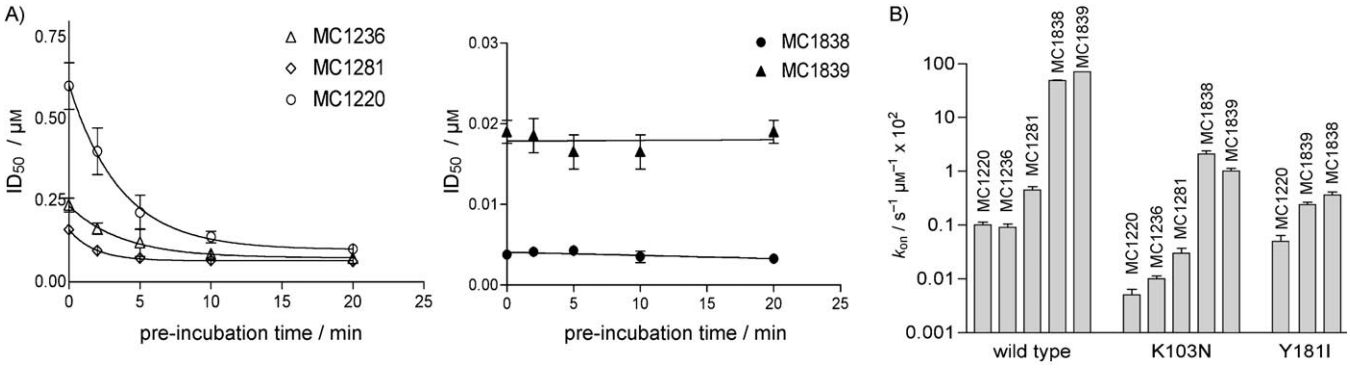

Figure 2. Binding properties of *N*,*N*-DABO derivatives. A) Variation of the apparent inhibition potency (ID_{50}) against wild-type HIV-1 RT for MC1236 (△), MC1281 (◇), MC1220 (○), MC1838 (●), and MC1839 (▲) as a function of pre-incubation time. Reactions were performed as described in the Experimental Section. Values are the mean of three replicates, and error bars indicate ±SD. Owing to the differences in the absolute ID_{50} values, the results are presented in two different graphs for better clarity. B) Association rates (k_{on}) of the various compounds to the free enzyme state of wild-type HIV-1 RT and the K103N and Y181I mutants. Kinetic constants were determined as described in the Experimental Section. Data are plotted on a $\log_{10}$ scale due to the differences in the absolute k_{on} values. Values are the mean of three replicates, and error bars indicate ±SD.

Table 3. Kinetic parameters for the interaction of *N*,*N*-DABOs with the various catalytic states of wild-type and mutated HIV-1 RT forms.

		Free [E]		Binary [E·NA]		Ternary [E·NA·dTTP]	
Compd	K_i [μM]	k_{on} [$\times 10^2 s^{-1} \mu M^{-1}$][a]	k_{off} [$\times 10^2 s^{-1}$]	k_{on} [$\times 10^2 s^{-1} \mu M^{-1}$]	k_{off} [$\times 10^2 s^{-1}$]	k_{on} [$\times 10^2 s^{-1} \mu M^{-1}$]	k_{off} [$\times 10^2 s^{-1}$]
Wild-type RT							
MC1220	0.1 ± 0.03	0.03 ± 0.002	0.003 ± 0.001	0.03 ± 0.002	0.003 ± 0.001	0.03 ± 0.002	0.003 ± 0.001
MC1236	0.07 ± 0.01	0.08 ± 0.01	0.006 ± 0.001	0.08 ± 0.01	0.006 ± 0.001	0.08 ± 0.01	0.006 ± 0.001
MC1281	0.06 ± 0.01	0.4 ± 0.02	0.02 ± 0.003	0.4 ± 0.02	0.02 ± 0.003	0.4 ± 0.02	0.02 ± 0.003
MC1838	0.0032 ± 0.0002	44.7 ± 4.1	0.14 ± 0.01	45.3 ± 4.3	0.15 ± 0.01	49.2 ± 4.7	0.16 ± 0.01
MC1839	0.0175 ± 0.001	57.1 ± 4.3	1.00 ± 0.08	176.4 ± 16.8	3.1 ± 0.3	70.3 ± 7.1	1.2 ± 0.1
K103N							
MC1220	0.5 ± 0.1	0.005 ± 0.001	0.025 ± 0.001	0.005 ± 0.001	0.025 ± 0.001	0.005 ± 0.001	0.025 ± 0.001
MC1236	0.6 ± 0.06	0.01 ± 0.003	0.006 ± 0.001	0.01 ± 0.003	0.006 ± 0.001	0.01 ± 0.003	0.006 ± 0.001
MC1281	10 ± 1	0.034 ± 0.004	0.34 ± 0.04	0.034 ± 0.004	0.34 ± 0.04	0.034 ± 0.004	0.34 ± 0.04
MC1838	1 ± 0.09	2.2 ± 0.2	2.2 ± 0.2	1.3 ± 0.1	1.3 ± 0.1	0.2 ± 0.02	0.2 ± 0.02
MC1839	0.75 ± 0.078	1 ± 0.48	0.75 ± 0.03	2.2 ± 0.4	1.7 ± 0.3	0.22 ± 0.01	0.16 ± 0.01
Y181I							
MC1220	4 ± 0.5	0.05 ± 0.002	0.2 ± 0.002	0.05 ± 0.002	0.2 ± 0.002	0.5 ± 0.002	0.2 ± 0.002
MC1838	6 ± 0.5	0.24 ± 0.02	1.4 ± 0.09	0.08 ± 0.01	0.48 ± 0.05	0.02 ± 0.003	0.13 ± 0.01
MC1839	0.42 ± 0.04	0.36 ± 0.04	0.15 ± 0.02	0.63 ± 0.4	0.27 ± 0.09	0.07 ± 0.01	0.03 ± 0.007

[a] Kinetic parameters were determined as described in the Experimental Section. Values are the mean of three independent estimates ± SD.

data indicate that the 2-Cl-6-F derivatives with two methyl groups at the pyrimidine C5 and benzylic positions make more stable interactions with the NNBS of the mutated enzymes. This could be a result of both the flexibility of these compounds that imparts greater conformational freedom to respond to changes in the NNBS caused by mutations and to more favorable π-stacking interactions between the Y188 side chain and the 2-Cl-6-F substitution than with 2,6-F_2.

2-Cl-6-F-*N*,*N*-DABO derivatives have varied selectivity for the three catalytic states of mutated HIV-1 RT

We next compared the k_{on} and k_{off} values of the 2-Cl-6-F-*N*,*N*-DABOs MC1838 and MC1839 for the various states of HIV-1 RT along its reaction pathway: from free enzyme, to the binary complex between RT and the nucleic acid substrate, to the ternary complex between RT, the nucleic acid, and nucleotide substrates.

As reported in Table 3, no significant differences in the k_{on} and k_{off} rates of the compounds among the various states of wild-type HIV-1 RT were observed. However, in the case of the K103N and Y181I mutants, both compounds showed higher k_{on} values for the free enzyme and the binary complex than for the ternary complex (Figure 3 A). On the other hand, k_{off} values were significantly lower for the ternary complex than for the other enzymatic states (Figure 3 B). The proposed mode of binding is depicted in Figure 3 C. The 2-Cl-6-F-*N*,*N*-DABOs MC1838 and MC1839 quickly associate with free enzyme (E) or RT in complex with the nucleic acid substrate (E·NA), but slowly (as indicated by the dashed arrow) to the ternary complex of the enzyme with both substrates (E·NA·dNTP). The resulting enzyme–inhibitor (E·I) or enzyme–inhibitor–nucleic acid (E·I·NA) complexes are, however, in rapid equilibrium with the free inhibitor (I) and the E and E·NA enzymatic states, as indicated by the double arrows. However, upon binding of the dNTP substrate, the resulting E·I·NA·dNTP complex becomes stable and only very slowly reverts to the E·NA·dNTP ternary complex (dashed arrow). The compounds MC1838 and MC1839 are the first NNRTIs to show this peculiar mechanism of action and specifically toward mutated HIV-1 RT forms.

Conclusions

In this work we have presented the characterization of the mode of action of a novel class of *N*,*N*-DABO derivatives, the 2-Cl-6-F-*N*,*N*-DABOs. Starting from the observation that 2,6-F_2-*N*,*N*-DABO derivatives showed high antiviral potencies, but were still limited by a very low association rate to HIV-1 RT, we developed the 2-Cl-6-F-*N*,*N*-DABOs. These compounds show highly improved association rates toward HIV-1 RT wild-type and mutated forms. Moreover, analysis of their binding kinetics revealed a preferential association with mutated forms of HIV-1 RT in either the unbound state (free enzyme) or in complex with the nucleic acid substrate (binary complex). In contrast, their interaction with the mutated enzymes is greatly stabilized by binding of the nucleotide to the enzyme, resulting in very low dissociation rates of the inhibitor from the viral RT. These novel properties can be exploited to design NNRTIs that specifically target drug-resistant forms of HIV-1 RT.

Experimental Section

Chemistry

General: Melting points were determined on a Büchi 530 melting point apparatus and are uncorrected. IR spectra (KBr) were recorded on a PerkinElmer Spectrum One instrument. ^{1}H NMR spectra were recorded at 400 MHz on a Bruker AC 400 spectrometer; chemical shifts are reported in δ (ppm) relative to the internal ref-

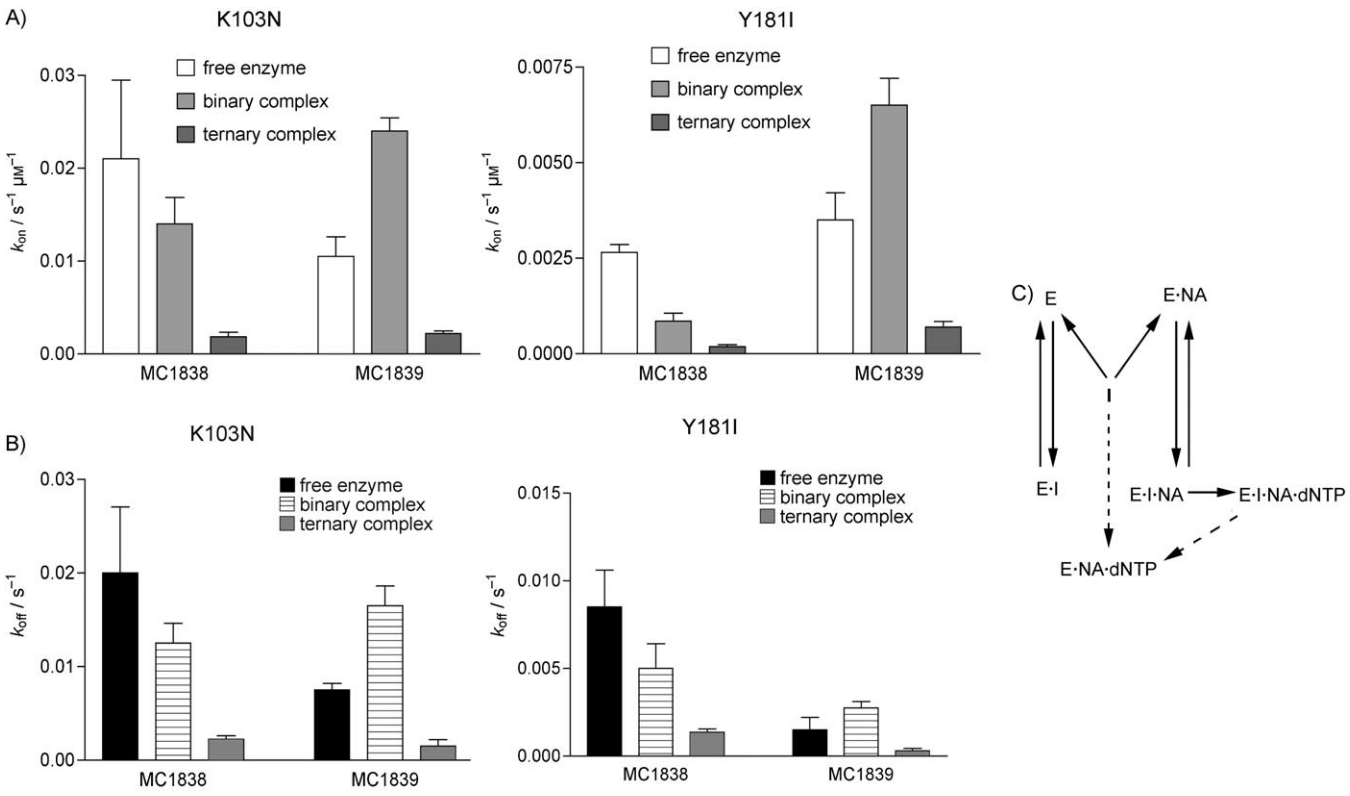

Figure 3. Interaction of 2-Cl-6-F-*N*,*N*-DABOs with mutant HIV-1 RT forms. Comparison of the A) k_{on} and B) k_{off} rates listed in Table 3 of 2-Cl-6-F-*N*,*N*-DABOs for the various catalytic states of HIV-1 RT K103N and Y181I, as indicated. C) Hypothetical simplified scheme for the interaction of 2-Cl-6-F-*N*,*N*-DABOs with HIV-1 RT; E = enzyme, NA = nucleic acid, dNTP = deoxynucleotide triphosphate. See text for details.

erence tetramethylsilane. All compounds were routinely checked by TLC and ^{1}H NMR. TLC was performed on aluminum-backed silica gel plates (Merck DC, Alufolien Kieselgel 60 F_{254}), with spots visualized by UV light. All solvents were reagent grade and, when necessary, were purified and dried by standard methods. Concentration of solutions after reactions and extractions involved the use of a rotary evaporator operating at ~20 Torr. Organic solutions were dried over anhydrous Na_2SO_4. Analytical results are within ±0.40% of theoretical values. All chemicals were purchased from Aldrich Chimica, Milan (Italy) or from Lancaster Synthesis GmbH, Milan (Italy), and were of the highest purity.

2-(2-chloro-6-fluorophenyl)propionic acid (2): A solution of diethylamine (2.5 mL, 24.2 mmol) in dry THF (5 mL) was added dropwise at −78 °C to a solution of butyllithium (19.4 mL of 2.5 M solution in *n*-hexane, 48.4 mmol) in dry THF (10 mL), and the resulting mixture was stirred for 0.5 h at 0 °C. A solution of 2-chloro-6-fluorophenylacetic acid (4.15 g, 22.0 mmol) in anhydrous THF (5 mL) was added dropwise at −78 °C to the mixture. After 0.5 h at 0 °C, a solution of methyl iodide (3.43 g, 1.5 mL, 24.2 mmol) in dry THF (5 mL) was added at −78 °C. The mixture was stirred and gradually warmed from −78 °C to room temperature over 1 h, and then poured into H_2O (150 mL) and extracted with EtOAc (3×50 mL). The aqueous layer was acidified with concentrated HCl at 0 °C and extracted with EtOAc (4×50 mL). The combined organic layers were washed with brine to neutral pH and dried with anhydrous Na_2SO_4. Evaporation of solvent gave the crude acidic fraction that was purified by column chromatography (silica gel, EtOAc/$CHCl_3$ 1:5); mp: 84–87 °C (*n*-hexane). Yield 91.8%; ^{1}H NMR ($CDCl_3$): δ = 1.34 (d, J = 7.2 Hz, 3H, $CHCH_3$), 4.13 (q, J = 7.2 Hz, 1H, $CHCH_3$), 7.19 (m, 1H, C4-Ar-*H*), 7.30 ppm (m, 2H, C3–5-Ar-*H*); Anal. C, H, Cl, F.

General procedure for the preparation of ethyl-(2-chloro-6-fluorophenyl)oxoalkanoates (3–6): *Example: ethyl-4-(2-chloro-6-fluorophenyl)-3-oxopentanoate (**5**).* Triethylamine (9.0 mL, 64.7 mmol) and $MgCl_2$ (4.82 g, 50.5 mmol) were added to a stirred suspension of potassium malonate monoethylester (7.23 g, 42.4 mmol) in dry CH_3CN (80 mL), and stirring was continued at room temperature for 2 h. Then, a solution of the 2-(2-chloro-6-fluorophenyl)propionic imidazolide in the same solvent (28 mL), prepared 15 min previously by reaction between 2-(2-chloro-6-fluorophenyl)propionic acid (4.10 g, 20.2 mmol) and *N*,*N*′-carbonyldiimidazole (3.90 g, 24.2 mmol) in CH_3CN (28 mL), was added. The reaction mixture was stirred overnight at room temperature and was then heated at reflux for 2 h. After the mixture was cooled, 13% HCl (180 mL) was cautiously added while the temperature was kept below 25 °C, and the resulting clear mixture was stirred for a further 15 min. The organic layer was separated and evaporated, and the residue was treated with EtOAc (100 mL). The aqueous layer was extracted with EtOAc (3×60 mL), and the organic phases were collected, washed with a saturated solution of $NaHCO_3$ (3×60 mL) and brine (3×60 mL), dried, and concentrated to give pure desired product as a yellow oil, which was directly used in the following step. Yield: 86.4%; ^{1}H NMR ($CDCl_3$): δ = 1.21 (t, J = 7.1 Hz, 3H, $COCH_2CH_3$), 1.42 (d, J = 6.9 Hz, 3H, $CHCH_3$), 3.34 (m, 2H, $COCH_2CO$), 4.11 (m, 2H, $COCH_2CH_3$), 4.29 (q, J = 6.9 Hz, 1H, $CHCH_3$), 7.01 (m, 1H, C4-Ar-*H*), 7.22 (m, 2H, C3,5-Ar-*H*).

The same procedure allowed us to obtain the β-oxoesters **3**, **4**, and **6**: ethyl-4-(2-chloro-6-fluorophenyl)-3-oxobutyrate (**3**), mp: 48–50 °C (*n*-hexane), yield 92%; ethyl-4-(2-chloro-6-fluorophenyl)-2-methyl-3-oxobutyrate (**4**), oil, yield 65%; ethyl-4-(2-chloro-6-fluorophenyl)-2-methyl-3-oxopentanoate (**6**), oil, yield 78.6%.

General procedure for the preparation of 6-[(2-chloro-6-fluorophenyl)alkyl]-2-(dimethylamino)pyrimidin-4(3*H*)-ones (MC1778, MC1784, MC1838, MC1839): *Example: 6-[1-(2-chloro-6-fluorophenyl)ethyl]-2-dimethylamino-5-methylpyrimidin-4(3*H*)-one (MC1839).* Sodium metal (0.499 g, 0.022 g-atom) was dissolved in 11.5 mL absolute EtOH, and 1,1-dimethylguanidine hydrogensulfate (1.27 g, 9.3 mmol) and ethyl-4-(2-chloro-6-fluorophenyl)-2-methyl-3-oxopentanoate **6** (1.78 g, 6.2 mmol) were added to the clear solution. The mixture was heated at reflux for 5 h. After cooling, the solvent was distilled in vacuo at 40–50 °C, and the residue was dissolved in H_2O (20 mL), neutralized with 2 N HCl, and extracted with EtOAc (3×25 mL). The organic extracts were washed with brine (3× 20 mL), dried, and evaporated in vacuo, and the residue was purified by crystallization from EtOAc; mp: 187–190 °C (EtOAc). Yield 73%; ^{1}H NMR ([D$_6$]DMSO): $\delta = 1.50$ (d, $J = 5.4$ Hz, 3H, ArCHCH_3), 1.70 (s, 3H, C5-CH_3), 2.94 (s, 6H, NCH_3), 4.53 (q, $J = 5.4$ Hz, 1H, ArC*H*CH$_3$), 7.15 (m, 1H, C4-Ar-*H*), 7.24 (m, 1H, C3,5-Ar-*H*), 10.98 (s 1H, N*H*).

According to the described procedure MC1778, MC1784, and MC1838 were obtained: 6-(2-chloro-6-fluorobenzyl)-2-dimethylaminopyrimidin-4(3*H*)-one (MC1778), mp: 219–221 °C (MeCN), yield 66%; 6-(2-chloro-6-fluorobenzyl)-2-dimethylamino-5-methylpyrimidin-4(3*H*)-one (MC1784), mp: 240–240.5 °C (MeCN), yield 69%; 6-[1-(2-chloro-6-fluorophenyl)ethyl]-2-dimethylaminopyrimidin-4(3*H*)-one (MC1838), mp: 190–192 °C (MeCN), yield 71%.

Cell-based anti-HIV assays

The biological activity of the compounds was tested in the lymphoid MT-4 cell line (received from the NIH AIDS Reagent Program) against the wild-type HIV-1 NL4-3 strain and three different HIV-1 strains, as described earlier.[16,17] Briefly, MT-4 cells were infected with the appropriate HIV-1 strain (or mock infected to determine cytotoxicity) in the presence of various drug concentrations. At day five post-infection, a tetrazolium-based colorimetric method (MTT assay) was used to evaluate the number of viable cells. The IRLL98 HIV-1 strain contains the following mutations in the RT coding sequence:[18] M41L, D67N, Y181C, M184V, R211K, T215Y (conferring resistance to NRTIs) and mutations K101Q, Y181C, G190A (conferring resistance to NNRTIs). The HIV-1 strains containing the multi-NNRTI mutation, K103N, or the Y188L mutant were received from the Medical Research Council Centralised Facility for AIDS Reagents, Herfordshire, UK.

Biochemistry

Chemicals: All reagents were of analytical grade and purchased from Sigma–Aldrich (St. Louis, MO, USA), Merck Sharp & Dohme (Readington, NJ, USA), ICN (Research Products Division, Costa Mesa, CA, USA), or AppliChem GmbH (Darmstadt, Germany). Radioactive 2′-deoxythymidine-5′-triphosphate [^{3}H]dTTP (40 Ci mmol^{-1}) was purchased from Amersham BioSciences (GE Healthcare, Buckinghamshire, UK), and unlabeled dNTPs were from Boehringer Ingelheim GmbH (Ingelheim, Germany). GF/C filters were provided by Whatman Ltd. (Maidstone, UK).

Nucleic acid substrates

The homopolymer poly(rA) and the oligomer oligo(dT)$_{12-18}$ (Pharmacia & Upjohn Inc. (Pfizer, Peapack, NJ, USA)) were mixed at weight ratios in nucleotides of 10:1 with 25 mM Tris HCl (pH 8.0) containing 22 mM KCl, heated at 70 °C for 5 min and then slowly cooled to room temperature.

Expression, purification, and cloning of recombinant HIV-1 RT forms

Recombinant heterodimeric RT, either wild type or the K103N, L100I, and Y181I variants, were expressed and purified as described.[13] Briefly, the HIV-1 RT gene fragment spanning codons 2–261 from pHXB2D2–261RT constructs carrying K103N, L100I, and Y181I mutations was amplified by PCR, digested with restriction endonucleases AccI and PvuII, and cloned into the expression plasmid p6HRT (ΔXho1/Bgl2), containing the wild-type RT gene. The resulting p6HRT expression vectors with K103N, L100I, and Y181I mutations were used for production in *E. coli* (BL21), and subsequent purification of the recombinant His-tagged RT enzymes was carried out in a fast protein liquid chromatography (FPLC) system with a Ni-NTA superflow column (Qiagen, USA).[19] All enzymes were purified to >95% purity, as confirmed by sodium dodecyl sulfate polyacrylamide gel electrophoresis and Gelcode Blue stain, and had specific activity on poly(rA)/oligo(dT). One unit of DNA polymerase activity corresponds to the incorporation of 1 nmol dNMP into acid-precipitable material in 60 min at 37 °C. Western blotting confirmed the identity of the polypeptides present in the final preparation with anti-RT monoclonal antibodies.

HIV-1 RT RNA-dependent DNA polymerase activity assay

Poly(rA)/oligo(dT) was used as a template for the RNA-dependent DNA polymerase activity of wild-type or mutant forms of HIV-1 RT. For the activity assay, a final reaction volume of 25 μL contained TDB buffer (50 mM Tris-HCl (pH 8.0), 1 mM dithiothreitol, 0.2 mg mL^{-1} bovine serum albumin, 2% glycerol), 10 mM $MgCl_2$, 0.5 mg poly(rA)/oligo(dT) (10:1, 0.3 mM 3′-OH ends), 10 mM [^{3}H]dTTP (1 Ci mmol^{-1}). This mixture was introduced into tubes containing aliquots of various RT concentrations (5–10 nM). After incubation at 37 °C for the indicated time, 20 μL from each reaction tube were spotted on GF/C glass fiber filters and immediately immersed in 5% ice-cold trichloroacetic acid (TCA, AppliChem GmbH, Darmstadt, Germany). Filters were washed three times with 5% TCA, once with EtOH for 5 min, and then dried. EcoLume Scintillation cocktail (ICN, Research Products Division, Costa Mesa, CA, USA) was added to detect the acid-precipitable radioactivity with a PerkinElmer Trilux MicroBeta 1450 scintillation counter.

Steady-state kinetics and inhibition assays

Steady-state kinetics assays were performed to evaluate the activity of HIV-1 RT in the presence of fixed concentrations of the selected inhibitors and variable concentrations of one of the two substrates (either poly(rA)/oligo(dT) or [^{3}H]dTTP), while the other was maintained at saturating concentration. [^{3}H]dTTP concentrations varied between 0.2 and 20 μM, while poly(rA)/oligo(dT) concentrations ranged from 10 to 40 nM. These experiments led to the determination of V_{max}, K_M, and k_{cat} parameters from Michaelis–Menten curves. The true inhibitor dissociation constant (K_i) values were derived according to the equation for a fully noncompetitive mechanism of inhibition, from the variations of the K_M and V_{max} values as a function of the inhibitor concentrations according to the equation:

$$K_i = I/[(V_{max}/V_p)-1] \quad (1)$$

for which V_p is the apparent maximal velocity of the reaction in the presence of any given concentration of the inhibitor *I*.

Kinetics of inhibitor binding

Kinetics experiments for inhibitor binding were carried out as described previously. Briefly, HIV-1 RT (20–40 nM) was incubated for 2 min at 37 °C in a final volume of 4 μL in the presence of TDB buffer, with 10 mM $MgCl_2$ alone or with 100 nM 3′-OH ends (for the formation of the RT–template complex), or in the same mixture complemented with 10 μM unlabeled dTTP (for the formation of the RT–template–dNTP complex). The inhibitor to be tested was then added to a final volume of 5 μL at a concentration at which $[E_i]/[E_0] = [1-1/(1+[I]/K_i)] > 0.9$. Then, 145 μL of a mix containing TDB buffer, 10 mM $MgCl_2$, and 10 μM [^{3}H]dTTP (5 Ci mmol^{-1}) was added at various time points. After an additional 10 min incubation at 37 °C, 50 μL aliquots were spotted on GF/C filters, and acid-precipitable radioactivity was measured as described for the HIV-1 RT RNA-dependent DNA polymerase activity assay. The V_t/V_0 ratio, which represents the normalized difference between the amount of dTTP incorporated at time zero and at various time points V_t, was then plotted against time. The apparent binding rate (k_{app}) values were determined by fitting the experimental data to the single-exponential equation:

$$V_t/V_0 = e^{-k_{app}\,t} \quad (2)$$

in which t = time. If $[E]_0$ is the input enzyme concentration, $[E]_t$ is the enzyme available for the reaction at time t, and $[E{\cdot}I]_t$ is the enzyme bound to the inhibitor at time t, it follows that:

$$[E]_t = [E]_0 - [E \cdot I]_t \quad (3)$$

because $V_0 = k_{cat}[E]_0$ and $V_t = k_{cat}[E]_t$, then $V_t/V_0 = 1-[E{\cdot}I]_t/[E]_0$. Thus, the V_t/V_0 value is proportional to the fraction of enzyme bound to the inhibitor. The true association (k_{on}) and dissociation (k_{off}) rates were calculated from the equations:

$$k_{app} = k_{on}([I] + K_i) \quad (4)$$

$$k_{off} = k_{on}K_i \quad (5)$$

Data analysis and statistics

Data obtained were analyzed by nonlinear regression analysis using GraphPad Software (San Diego, CA, USA).

Acknowledgements

This work was partially supported by the VI Programma Nazionale AIDS Grant no. 40G.36 to G.M., the Spanish MEC (project BFI2006-00966) to J.A.E., and by the EU grant LSHP-CT-2006-037257 ExcellentHit to G.M.

Keywords: antiviral agents · HIV-1 · medicinal chemistry · reverse transcriptase

[1] G. S. Maga, *Curr. Drug Metab.* **2002**, *3*, 73–95.
[2] M. Artico, *Drugs Future* **2002**, *27*, 159–175.
[3] M. Artico, S. Massa, A. Mai, M. E. Marongiu, G. Piras, E. Tramontano, P. La Colla, *Antiviral Chem. Chemother.* **1993**, *4*, 361–368.
[4] E. Tramontano, M. E. Marongiu, A. De Montis, A. G. Loi, M. Artico, S. Massa, A. Mai, P. La Colla, *New Microbiol.* **1994**, *17*, 269–279.
[5] S. Massa, A. Mai, M. Artico, G. Sbardella, E. Tramontano, A. G. Loi, P. Scano, P. La Colla, *Antiviral Chem. Chemother.* **1995**, *6*, 1–8.
[6] A. Mai, M. Artico, G. Sbardella, S. Massa, A. G. Loi, E. Tramontano, P. Scano, P. La Colla, *J. Med. Chem.* **1995**, *38*, 3258–3263.
[7] A. Mai, M. Artico, G. Sbardella, S. Quartarone, S. Massa, A. G. Loi, A. De Montis, F. Scintu, M. Putzolu, P. La Colla, *J. Med. Chem.* **1997**, *40*, 1447–1454.
[8] A. Mai, M. Artico, G. Sbardella, S. Massa, E. Novellino, G. Greco, A. G. Loi, E. Tramontano, M. E. Marongiu, P. La Colla, *J. Med. Chem.* **1999**, *42*, 619–627.
[9] A. Mai, G. Sbardella, M. Artico, R. Ragno, S. Massa, E. Novellino, G. Greco, A. Lavecchia, C. Musiu, M. La Colla, C. Murgioni, P. La Colla, R. Loddo, *J. Med. Chem.* **2001**, *44*, 2544–2554.
[10] R. Ragno, A. Mai, S. Sbardella, M. Artico, S. Massa, C. Musiu, M. Mura, T. Marceddu, A. Cadeddu, P. La Colla, *J. Med. Chem.* **2004**, *47*, 928–934.
[11] A. Mai, M. Artico, R. Ragno, G. Sbardella, S. Massa, C. Musiu, M. Mura, F. Marturana, A. Cadeddu, G. Maga, P. La Colla, *Bioorg. Med. Chem.* **2005**, *13*, 2065–2077.
[12] R. Ragno, S. Frasca, F. Manetti, A. Brizzi, S. Massa, *J. Med. Chem.* **2005**, *48*, 200–212.
[13] R. Cancio, A. Mai, D. Rotili, M. Artico, G. Sbardella, I. Clotet-Codina, J. A. Esté, E. Crespan, S. Zanoli, U. Hübscher, S. Spadari, G. Maga, *ChemMedChem* **2007**, *2*, 445–448.
[14] A. Mai, M. Artico, D. Rotili, D. Tarantino, I. Clotet-Codina, M. Armand-Ugón, R. Ragno, S. Simeoni, G. Sbardella, M. B. Nawrozkij, A. Samuele, G. Maga, J. A. Esté, *J. Med. Chem.* **2007**, *50*, 5412–5424.
[15] M. G. Quaglia, A. Mai, G. Sbardella, M. Artico, R. Ragno, S. Massa, D. Del Piano, G. Setzu, S. Doratiotto, V. Cotichini, *Chirality* **2001**, *13*, 75–80.
[16] G. Moncunill, M. Armand-Ugón, E. Pauls, B. Clotet, J. A. Esté, *AIDS* **2008**, *22*, 23–31.
[17] G. Moncunill, M. Armand-Ugón, I. Clotet-Codina, E. Pauls, E. Ballana, A. Llano, B. Romagnoli, J. W. Vrijbloed, F. O. Gombert, B. Clotet, S. De Marco, J. A. Esté, *Mol. Pharmacol.* **2008**, *73*, 1264–1273.
[18] M. Cabana, B. Clotet, M. A. Martinez, *J. Med. Virol.* **1999**, *59*, 480–490.
[19] N. Abdullah, H. A. Chase, *Biotechnol. Bioeng.* **2005**, *92*, 501–513.

Received: February 21, 2008
Revised: April 11, 2008
Published online on May 8, 2008

